BIOCHEMISTRY
including biophysical chemistry & molecular biology

Article

pubs.acs.org/biochemistry

Binding Modes and Functional Surface of Anti-mammalian Scorpion α-Toxins to Sodium Channels

Rong Chen* and Shin-Ho Chung

Research School of Biology, Australian National University, Canberra, ACT 0200, Australia

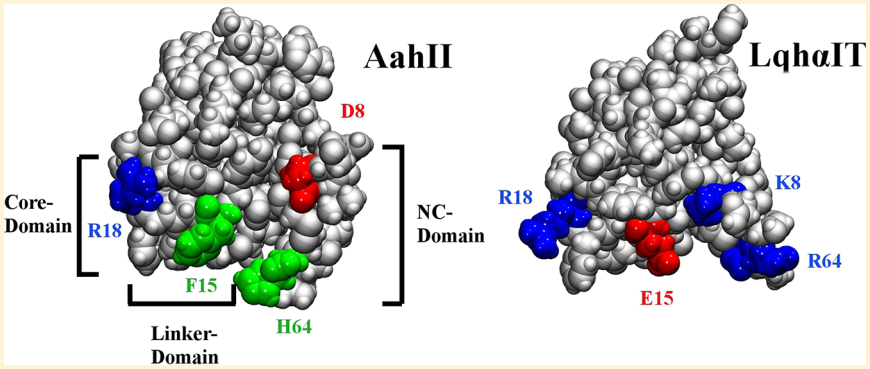

ABSTRACT: Scorpion α-toxins bind to the voltage-sensing domains of voltage-gated sodium (Na_V) channels and interfere with the inactivation mechanisms. The functional surface of α-toxins has been shown to contain an NC-domain consisting of the five-residue turn (positions 8−12) and the C-terminus (positions 56−64) and a core-domain centered on the residue 18. The NC- and core-domains are interconnected by the linker-domain (positions 8−18). Here with atomistic molecular dynamics simulations, we examine the binding modes between two α-toxins, the anti-mammalian AahII and the anti-insect LqhαIT, and the voltage-sensing domain of rat $Na_V1.2$, a subtype of Na_V channels expressed in nerve cells. Both toxins are docked to the extracellular side of the voltage-sensing domain of $Na_V1.2$ using molecular dynamics simulations, with the linker-domain assumed to wedge into the binding pocket. Several salt bridges and hydrophobic clusters are observed to form between the NC- and core-domains of the toxins and $Na_V1.2$ and stabilize the toxin−channel complexes. The binding modes predicted are consistent with available mutagenesis data and can readily explain the relative affinities of AahII and LqhαIT for $Na_V1.2$. The dissociation constants for the two toxin−channel complexes are derived, which compare favorably with experiment. Our models demonstrate that the functional surface of anti-mammalian scorpion α-toxins is centered on the linker-domain, similar to that of β-toxins.

Voltage-gated sodium (Na_V) channels, responsible for the rising phase of action potential, are widely distributed in nerve and muscle cells. Upon membrane depolarization, Na_V channels open and then inactivate rapidly. The structure of Na_V channels is rather complex. Eukaryotic Na_V channels are integral proteins containing four homologous subunits (I−IV); each subunit consists of a voltage-sensing (VS) domain formed by four helices S1−S4 and a pore domain formed by S5 and S6 helices. Several classes of polypeptide toxins that affect the VS movement and interfere with the gating mechanism of Na_V channels have been isolated from venoms of scorpions and cone snails. For example, scorpion β-toxins trap the VS-domain in the open state such that the channel opens at less depolarized voltages, whereas δ-conotoxins and scorpion α-toxins can induce slow and incomplete inactivation of Na_V channels, resulting in prolonged action potentials.[1−6] These toxins have been fruitfully utilized for elucidating the gating mechanisms of Na_V channels. Understanding their mechanisms of action may potentially lead to the discovery of novel insecticides or pharmaceutical agents.[7,8]

Scorpion α-toxins are polypeptides consisting of 60−70 amino acids.[9] The structure of α-toxins is highly conserved, with four disulfide bridges cross-linking one α-helix and three antiparallel β-sheet strands.[9−11] Various α-toxins selectively targeting mammalian or insect Na_V channels have been isolated.[9,12] For example, AahII[13,14] from *Androctonus australis hector* and LqhII[15,16] from *Leiurus quinquestriatus hebraeus* are two of the most potent α-toxins for Na_V channels in mammals, whereas LqhαIT[17] from *Leiurus quinquestriatus hebraeus* is selective for Na_V channels in insects. LqhII has been shown to be about 3 orders of magnitude more effective than LqhαIT for the rat $Na_V1.2$ channel.[15] The α-like toxins such as LqhIII,[18] on the other hand, are active for both mammalian and insect Na_V channels. AahII is different than LqhII in only two of the 64 residues it carries located at the N- and C-termini. The two terminal residues of AahII are valine and histidine, corresponding to isoleucine and arginine at the same positions of LqhII, respectively. Despite a high sequence identity of 97%, the affinities of AahII and LqhII for mammalian or insect Na_V channels can differ by up to 10-fold,[16] suggesting that the C-

Received: June 12, 2012
Revised: August 14, 2012
Published: September 12, 2012

terminal residue may be involved in binding.[14] LqhαIT shares about 50% sequence identity with AahII and LqhII (Figure 1A).

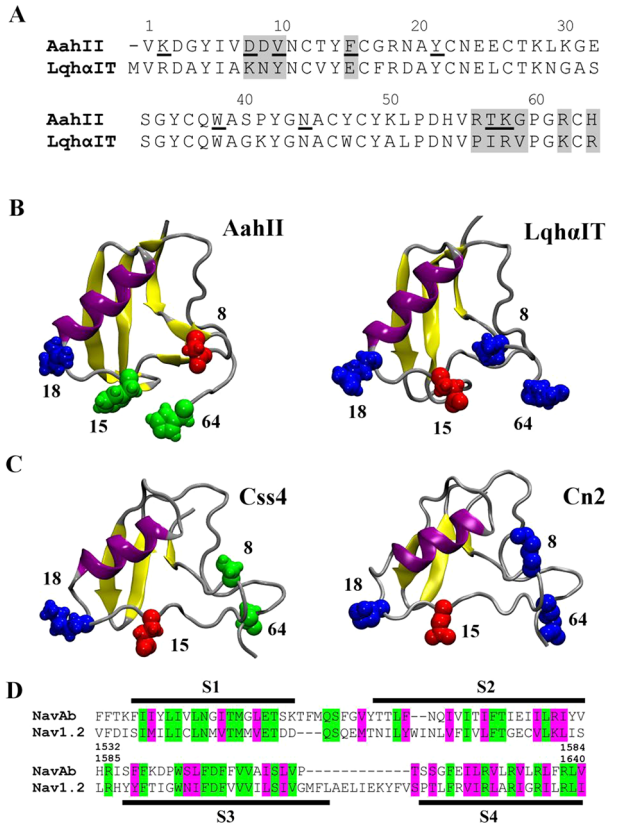

Figure 1. (A) Sequence alignment of two α-toxins, AahII and LqhαIT. The key different residues between AahII and LqhαIT are shaded. The residues of AahII likely involved in binding according to Kahn et al.[15] are highlighted with underscore. (B) The secondary structure of AahII[10] and LqhαIT.[11] Helices are shown in purple, β-sheet strands in yellow, and others in gray. The side chains of residues at positions 8 and 64 of the NC-domain, 18 of the core-domain, and 15 of the linker-domain are highlighted. Basic residues are colored in blue, acidic in red, and others in green. (C) The secondary structure of two anti-mammalian β-toxins, Css4 and Cn2.[52] The Css4 structure is modeled on Cn2. (D) A sequence alignment of Na_VAb and the IV VS domain of rat Na_V1.2. Numbering is that of Na_V1.2. Horizontal bars represent the four transmembrane helices S1−S4. Identical residues are highlighted in green and similar residues in purple.

The key different residues are from the NC-domain and the linker-domain, which have been found to largely determine the selectivity of these toxins.[15] The NC-domain consists of a five-residue turn (residues 8−12) and the C-terminal segment (residues 56−64), whereas the core-domain is formed by several residues spatially in close proximity to the residue at position 18.

The receptor site of scorpion α-toxins on Na_V channels has been determined experimentally. Tejedor and Catterall[19] found that a photoaffinity-labeled α-toxin showed competitive binding to Na_V channels with the antibodies specific for the amino acid sequences of the loop linking IS5 and IS6 helices, suggesting that the receptor site contains the subunit I.[19] Subsequently, using site-directed mutagenesis, Rogers et al.[20] demonstrated that the extracellular loop linking the S3 and S4 helices of the subunit IV also forms part of the receptor site for α-toxins. One glutamate residue at the extracellular end of the IVS3 helix (position 1613) was found to be particularly important.[20] The importance of this glutamate residue has been confirmed by Benzinger et al.,[21] Leipold et al.,[22] and Gur et al.[23] For example, Gur et al.[23] showed that replacing this glutamate residue with an aspartate transformed the sensitivity of rat Na_V1.2 to LqhαIT. More recently, it has been proposed that the extracellular segments of the VS domain of the subunit IV forms the primary receptor site for α-toxins, with the IS5-S6 linker forming the secondary receptor site.[24] The crystal structure of a bacterial Na_V channel[25] shows that the IVS1-S4 domain is in close proximity to the IS5-S6 domain in the presumably preopen state of the channel. Thus, on binding to the IVS1-S4 domain, a segment of the toxin could interact with the IS5-S6 domain.

The functional surface of α-toxins has also been examined experimentally using site-directed mutagenesis techniques. For example, Zilberberg et al.[26] found that several residues of the NC-domain and the core-domain of LqhαIT are critical in binding Na_V channels. Similar functional surface has been suggested by the results of Karbat et al.[27] and Kahn et al.[15] The core-domain and the NC-domain are interconnected by a loop between positions 8 and 18, which we refer to as the linker-domain. The pivotal role of the residue at position 15 in the linker-domain has been demonstrated,[15] suggesting that the linker-domain may also be important for toxin binding.

The secondary and tertiary structure of β-toxins is very similar to that of α-toxins, except that the two antiparallel β-sheet strands behind the α-helical segment of α-toxins are longer (Figure 1B,C). However, the primary sequences of α- and β-toxins are rather different, resulting in their different receptor sites and functional effects on Na_V channels. Scorpion β-toxins bind to the subunit II, rather than the subunit IV for α-toxins.[1] In our previous work,[28] we demonstrated that the functional surface of two anti-mammalian β-toxins contains the NC- and core-domain, and both the β-toxins wedge into the receptor site with the linker-domain. The functional surface of β-toxins we uncovered[28] overlaps well with that of α-toxins suggested by mutagenesis experiments.[15,26,27] Thus, the binding orientation may be conserved between scorpion α- and β-toxins, which we aim to demonstrate in this work.

Here with molecular dynamics (MD) simulations, we generate structural models of LqhαIT and AahII bound to the IVS1-S4 domain of rat Na_V1.2, respectively. AahII inhibits the inactivation of Na_V1.2 with nanomolar affinities, whereas LqhαIT is about 1000-fold less effective.[15] The structural models are compared to mutagenesis experiments, and further validated by free energy calculations, which show that the dissociation constants K_d derived agree with experiment. The models predicted are in support of the hypothesis that binding orientation is conserved between scorpion α- and β-toxins.

MATERIALS AND METHODS

Molecular Structures. We construct with SWISS-MODEL[29−31] a homology model of the isolated IVS1-S4 domain of rat Na_V1.2 (NCBI entry NP_036779.1), using the crystal structure of the bacterial Na_V channel Na_VAb (PDB ID 3RVY)[25] as a template. The sequence of the VS domain of the subunit IV of Na_V1.2 is ∼30% identical and ∼50% similar to that of Na_VAb (Figure 1D). A homology model is considered to be reliable if the sequence of the model is at least 30% identical to that of the template.[32] It has been demonstrated experimentally that the overall architecture of VS domains is highly conserved across cationic channels.[33] Moreover, the

dx.doi.org/10.1021/bi300776g | Biochemistry 2012, 51, 7775−7782

structure is observed to be stable over a simulation period of 30 ns when embedded in a lipid bilayer and a box of explicit water.

In the crystal structure of Na_VAb, the VS domain is believed to be in the activated state.[25] Thus, we have generated a model that is representative of an activated VS domain of $Na_V1.2$. Experimentally, the binding affinities of α-toxins for Na_V channels have been shown to be voltage dependent and decrease with depolarization.[4,24,34−36] It is unsure whether this voltage dependence is due to the toxins binding more readily to the resting-state channel[24] or other mechanisms such as slow inactivation of the channel during depolarization.[4,35,37] As the maximum effect of depolarization on the binding affinity of α-toxins is 1 order of magnitude,[34,35] it can be assumed that scorpion α-toxins bind strongly to the VS domains of sodium channels, regardless of the state of the VS domain.

The interactions between the toxins and the pore domain of the subunit I, which may be the secondary binding site of α-toxins,[24] are not considered in the present work, due to the poor sequence similarity between the pore domains of Na_VAb and $Na_V1.2$. The structures 1PTX[10] and 1LQH[11] are used for AahII and LqhαIT, respectively.

Molecular Dynamics Simulations. All MD simulations are performed using NAMD 2.8[38] at 1 atm and 300 K under periodic boundary conditions. The CHARMM36 force field is used to describe the interatomic interactions in the system.[39,40] The TIP3P model[41] is used for water molecules. The switch and cutoff distances for short-range interactions are set to 8.0 and 12.0 Å, respectively. The long-range electrostatic interactions are accounted for using the particle mesh Ewald method (grid spacing $\leq$1.0 Å). Bond lengths are maintained rigid with the SHAKE[42] and SETTLE[43] algorithms, allowing a time step of 2 fs to be used. Trajectories are saved every 20 ps for analysis.

Umbrella Sampling. To measure the dissociation constant for the predicted toxin−VS complexes, we construct a one-dimensional potential of mean force (PMF) profile for the unbinding of each of the toxins from the VS domain along the bilayer normal (z dimension). The starting structures of the umbrella windows spaced at 0.5 Å intervals are generated by pulling the toxin out from the binding site along the channel axis. The toxin backbone is maintained rigid using harmonic restraints during the pulling, whereas the backbone atoms of the channel are fixed. In subsequent umbrella sampling simulations, the backbones of toxin and VS domain are free to move.

The center of mass (COM) of the toxin backbone is restrained to the center of each umbrella window using a harmonic force constant of 30 kcal/(mol Å^2). The COM of the VS domain is at z = 0 Å. The COM of the toxin backbone is restrained in a cylinder of 8 Å in radius centered on the channel axis, using a flat-bottom harmonic restraint. This cylindrical restraint potential is always zero when the toxin is bound to the channel. Each umbrella window is simulated for 5.5 ns until the depth of the PMF profile changes by <0.5 kT over the last 1 ns. The toxin is observed to wander between the center and the edge of the cylinder multiple times in each umbrella window simulation, indicating that the sampling is adequate. The first 1 ns of each window is removed from data analysis. The weighted histogram analysis method is used to construct the PMF profile.[44] The dissociation constant (K_d) is derived using the equation[45,46]

$$K_d^{-1} = 1000\pi R^2 N_A \int_{z_{min}}^{z_{max}} \exp[-W(z)/kT]\, dz \quad (1)$$

where R is the radius of the cylinder (8 Å), N_A is Avogadro's number, z_{min} and z_{max} are the boundaries of the binding site along the reaction coordinate (z), $W(z)$ is the PMF, and kT assumes the usual significance.

RESULTS AND DISCUSSION

Docking of AahII to $Na_V1.2$. AahII inhibits the inactivation of $Na_V1.2$ with nanomolar affinities.[15] Here we show that AahII, when docked to the IVS1-S4 VS domain of $Na_V1.2$, forms several favorable electrostatic contacts with the VS domain.

We use MD simulation with biasing potential as a docking method. This docking method has been applied by Eriksson and Roux[47] to study the binding modes of agitoxin to the Shaker potassium channel. The docking procedure is detailed in Table 1. At the start of the simulation totaling 15 ns, the toxin

Table 1. Distance Restraints Applied during the Docking of AahII to the VS Domain of $Na_V1.2$ in a MD Simulation Totaling 15 ns

	flat-bottom distance restraint[b]		
simulation period (ns)	residue pairs	upper boundary (Å)	force constant (kcal/(mol Å^2))
0−2[a]	W38-L1568	6	2
	V10-A1631		
3−10	D9-R1626	5	1
	R18-E1613		
	K58-D1554		
	R62-E1551		

[a]Toxin backbone maintained rigid with harmonic restraints. [b]No distance restraints are applied during the simulation period of between 2 and 3 ns and between 10 and 15 ns.

AahII is released in water, about 20 Å above the extracellular side of the VS domain. The three-dimensional structures of the toxins and the VS domain are shown in Figure 2. The VS domain is embedded in a 2-oleoyl-1-palmitoyl-*sn*-glycero-3-phosphocholine bilayer, solvated with water and 0.2 M NaCl. The size of the simulation box is approximately 90 × 90 × 110 Å^3 at the start of the simulation.

Ideally, no biasing potential should be applied such that the toxin is allowed to bind to the VS spontaneously. However, such unbiased simulation requires a long time scale for the toxin to find the correct binding mode. To achieve the required degree of computational efficiency, flat-bottom distance restraints are applied to two toxin−VS residue pairs, labeled in Figure 3, during the first 2 ns. The restraining potential is zero when the distance between the COM of the residue pair is less than the upper boundary (Table 1). The two residue pairs are chosen according to the available experimental data on the functional surface of α-toxins[15,26,27] and the binding orientation of β-toxins previously uncovered.[28] On binding to the VS domain of Na_V channels, the linker-domain of β-toxins wedges into the receptor site, while the core-domain interacts with S2 and S3 helices and the NC-domain lies in the closest proximity to S1 and S4 helices.[28]

With the distance restraints applied, AahII is drawn to the receptor site rapidly within 2 ns (Figure 3). To prevent structural deformation in the toxin due to the restraining potential, the backbone of the toxin is maintained rigid with

dx.doi.org/10.1021/bi300776g | Biochemistry 2012, 51, 7775−7782

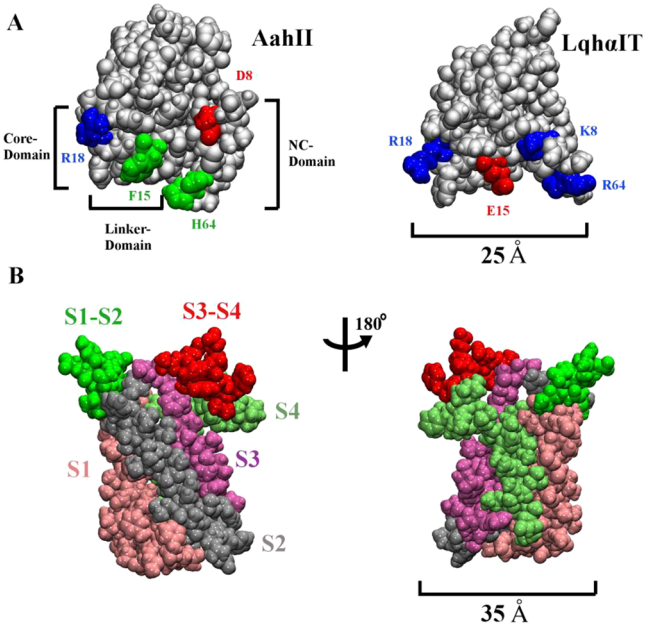

Figure 2. (A) Three-dimensional structures of AahII (left) and LqhαIT (right). (B) The IVS1-S4 domain of $Na_V1.2$ viewed from two perspectives.

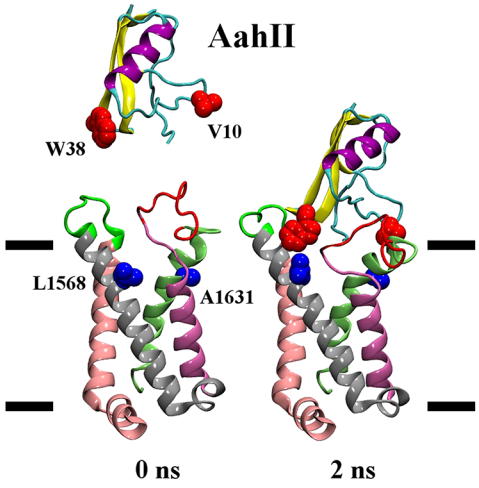

Figure 3. Position of AahII relative to the IVS1-S4 domain of $Na_V1.2$ at the start (left) and after 2 ns (right) of the docking simulation. The side chains of the residue pairs W38-L1568 and V10-A1631 to which distance restraints are applied are highlighted. Black horizontal bars represent the average position of the phosphate groups of lipids.

harmonic restraints in the first 2 ns. The cytoplasmic halves of the S1 and S4 helices are harmonically restraint throughout the simulation. No restraint is applied to other regions of the VS domain. Subsequently, the system is allowed to evolve for 1 ns with flexible toxin backbone and the two distance restraints released.

After the 1 ns equilibration, four toxin−VS residue pairs are identified. To speed up the formation of salt bridges and hydrogen bonds between these residue pairs, the distance restraint is applied to each residue pair. The four residue pairs and corresponding distance restraints applied are displayed in Table 1. The simulation is run for 7 ns with the restraints applied and then equilibrated for 5 ns with the distance restraints removed. Two of the residue pairs, Arg62-Glu1551 and Arg18-Glu1613, remain intact after the 5 ns unbiased simulation. However, the other two residue pairs, Lys58-Asp1554 and Asp9-Arg1626, are unstable and subsequently break. For example, Arg1626 is observed to form a salt bridge with the C-terminal carboxylate group rather than Asp9 of the toxin. The toxin does not appear to penetrate into the hydrophobic core of lipids. The final equilibrated structure is used for generating the starting configurations of the umbrella sampling windows.

To verify the stability of the final structure predicted by the docking simulation totaling 15 ns described above, three simulations each on a time scale of 30 ns starting from the docked complex are performed. The distance restraint is not applied in these simulations. The Arg62-Glu1551 salt bridge is unstable, as Arg62 is observed to switch between Glu1551 and Asp1554. However, the position of Arg62 relative to the VS does not change significantly. The other two salt bridges, Arg18-Glu1613 and His64(COO^-)-Arg1626, remain intact throughout the simulation period of 30 ns in all cases.

Docking of LqhαIT to $Na_V1.2$. The anti-insect α-toxin LqhαIT is about 1000-fold less effective to rat $Na_V1.2$ than AahII.[15] In line with this experimental measurement, we find that LqhαIT forms less favorable contacts with the VS domain than AahII, when docked to the receptor site on $Na_V1.2$.

To generate a model for the LqhαIT−$Na_V1.2$ VS complex, we replace AahII in the simulation box containing the final structural model of the AahII−$Na_V1.2$ VS complex with LqhαIT. The numbers of Na^+ and Cl^- ions are adjusted to maintain overall charge neutrality in the system. The LqhαIT-$Na_V1.2$ VS complex is then simulated for 30 ns without restraints.

After the 30 ns simulation, two salt bridges, Lys8-Glu1613 and Arg64-Arg1629, are formed in the LqhαIT−$Na_V1.2$ VS complex. Compared to that observed in the AahII−$Na_V1.2$ VS complex, the electrostatic interactions in the LqhαIT−$Na_V1.2$ VS complex appear to be less favorable. For example, the C-terminal carboxylate group of Arg64 forms less strong a salt bridge with the Arg1629 residue of the VS domain because the side chain of Arg64 carrying a positive charge is repelled by Arg1629, whereas the residue at position 64 of AahII is a neutral histidine. In addition, the five-residue turn in AahII (positions 8−12) carries two acidic residues, which are attracted by the arginine residues in the S4 helix. The weaker interactions between LqhαIT and the VS domain are reflected in its shallower PMF profile (see Figure 4).

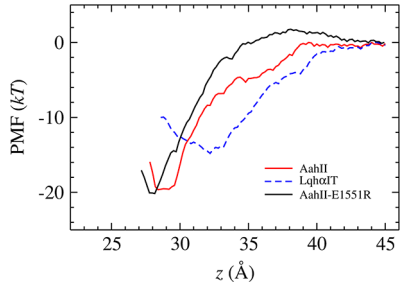

Figure 4. PMF profiles for the dissociation of AahII and LqhαIT from the VS domain of $Na_V1.2$ and AahII from the E1551R mutant $Na_V1.2$. The reaction coordinate (z) is parallel to the bilayer normal. The COM of the VS domain is at z = 0 Å. The random errors of all the PMF profiles are <0.4 kT.

dx.doi.org/10.1021/bi300776g | Biochemistry 2012, 51, 7775−7782

PMF Profiles. To predict the binding affinities of the toxins to the VS domain of $Na_V1.2$, we construct the PMF profiles for the dissociation of the toxins from the VS-domain and derive the dissociation constants K_d according to eq 1. The PMF profiles displayed in Figure 4 show that the free energy of binding is about −20 kT for AahII, ∼5 kT deeper than that of LqhαIT. The corresponding K_d values are 17 nM and 2 μM for AahII and LqhαIT, respectively, compared to the experimental values of 0.2−13 nM for AahII and ∼1 μM for LqhαIT.[13,15] The random errors of all PMF profiles are less than 0.4 kT, which would give an uncertainty of ∼2.2-fold in the K_d values derived. For detailed methods of deriving the random error of PMF profiles, see ref 28. The experimental values have an uncertainty of about 10-fold depending on voltage.[34] If the experimental K_d values are scaled by 10-fold, our predictions would still be within an order of magnitude of experimental values. We note that direct comparison between our predictions and experimental K_d values may be difficult because the isolated VS-domain rather than the whole channel protein is considered in our calculations. However, the contribution of the secondary receptor site which is ignored in our model to the PMF is expected to be insignificant. Thus, the K_d values derived from our models are in broad agreement with experiment, suggesting that the models predicted are good representations of the toxins at the bound state.

AahII−$Na_V1.2$ VS Interactions. Having shown that the complexes predicted are good representations of the toxins at the bound state, we identify the interacting residue pairs from the umbrella sampling simulations. The interacting residue pairs of the AahII−$Na_V1.2$ VS complex are of particular interest because AahII is one of the most potent α-toxins for $Na_V1.2$. The PMF profile displayed in Figure 4 for the dissociation of the AahII−$Na_V1.2$ VS complex shows that the window z = 29.0 Å represents the lowest energy. Therefore, the umbrella sampling simulation of this window is used to identify the interacting residue pairs, which are tabulated in Table 2. The average minimum distances between these residue pairs are also shown in the table. A representative configuration is shown in Figure 5.

As assumed in the docking simulation, the functional surface of AahII centers on the linker-domain. The Phe15 residue of the linker-domain forms a hydrophobic cluster with the Leu1611 of the S3 helix. The NC-domain of AahII is observed to interact with the S1 and S4 helices of the VS-domain. Two residues of the NC-domain, Asp8 and the carboxylate group of His64, form favorable electrostatic interactions with the Arg1626 residue of the S4 helix. Another residue of the NC-domain, Arg62, is in close proximity to the Asp1554 of the S1 helix. Note that Arg62 is in closer contact with the Glu1551 rather than Asp1554 of the S1 helix at the end of the 15 ns docking simulation. This suggests that the Arg62 is able to form salt bridges with different acidic residues that are clustered on the receptor site.

The core-domain of AahII, on the other hand, is found to interact primarily with the S2−S3 helices and the linker loop between the S3 and S4 helices. Specifically, Arg18 of AahII forms a salt bridge with the Glu1613 residue of the VS domain, with an average minimum distance of only 1.7 Å. The residue Trp38 of AahII interacts with a cluster of hydrophobic residues on the receptor site, including Tyr1564 and Trp1565 of the S2 helix. The residues Tyr21 and Asn44 are also observed to form close contacts with the channel (Table 2).

Table 2. Interacting Residue Pairs between AahII and $Na_V1.2$[a]

AahII		$Na_V1.2$		
domain	residue	domain	residue	av distance
NC-domain	D8	S4	R1626[d]	4.7 ± 1.7
	H64		R1626[d]	1.8 ± 0.4
	R62[b]	S1	D1554[d]	1.8 ± 0.3
	Y21[b]	S3−S4 linker	E1616[d]	4.2 ± 1.4
core-domain	R18[b]	S3−S4 linker	E1613[c]	1.7 ± 0.2
			E1616[d]	5.2 ± 2.0
	W38[b]	S2	Y1564[d]	2.6 ± 0.3
			W1565	2.7 ± 0.3
	N44[b]	S2	Y1564[d]	2.6 ± 0.3
linker-domain	F15[b]	S3−S4 linker	E1613[c]	5.9 ± 1.0
			L1611[c]	2.4 ± 0.2

[a]The minimum distances (Å) of each residue pair averaged over the last 4 ns are given. Standard deviations are shown. [b]Mutation of this residue reduces the toxin binding affinity by >5-fold according to the experiments of Kahn et al.[15] [c]Mutation of this residue reduces the toxin binding affinity by >5-fold according to the experiments of Rogers et al.,[20] Gur et al.,[23] and Wang et al.[24] [d]Mutation of this residue has no detectable effect on the toxin binding affinity in the experiments of Rogers et al.[20] and Wang et al.[24]

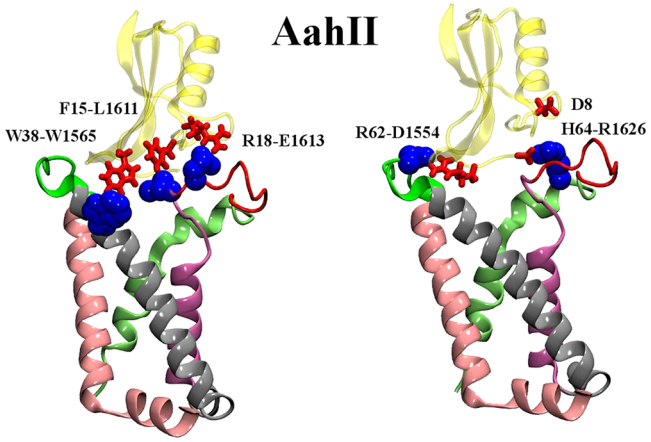

Figure 5. A representative configuration of AahII in complex with the IVS1−S4 VS-domain of $Na_V1.2$ from the 5 ns umbrella sampling simulation of the window z = 29.0 Å. The side chains of five key residue pairs are highlighted (toxin, red; channel, blue).

The interacting residue pairs identified from the AahII−$Na_V1.2$ VS complex are consistent with mutagenesis experiment. Both the NC-domain and core-domain, experimentally found to be important for binding,[26] are observed to form stable contacts with the VS-domain. However, two residues of the NC-domain, Lys2 and Lys58, the mutation of which to alanine causes >10-fold reduction in affinity,[15] are located just above the S1 and S4 helices but do not form salt bridges with the VS-domain in our model. In addition, the residue Thr57, the mutation of which to a serine causes about 2 orders of magnitude reduction in the binding affinity of Lqh2 to $Na_V1.2$,[15] is not in contact with the channel in our model. One possible explanation is that the mutation of these residues each causes significant conformational changes to the toxin. For example, it has been shown experimentally that the mutation of Lys58 to glutamate, valine, or isoleucine resulted in the toxin to adopt significantly different structure.[48] Another possible explanation would be that the two basic residues (Lys2 and

dx.doi.org/10.1021/bi300776g | Biochemistry 2012, 51, 7775−7782

Lys58) may interact favorably with the IS5-S6-domain, which is rich in acidic residues.

Comparison to a Previous Model. Recently, a model of LqhII in complex with the VS domain of $Na_V1.2$ has been proposed by Wang et al.,[24] which shows the same receptor site to our model displayed in Figure 5. However, a difference in the toxin functional surface is evident. In our model, both the core-domain and the NC-domain are bound to the receptor site. In contrast, in the model of Wang et al.,[24] the core-domain wedges into the receptor site but the NC-domain is in the water phase. It was hypothesized that the NC-domain may be in contact with the secondary receptor site (the pore domain of the subunit I), which was not included in the model.[24]

The discrepant models obtained by Wang et al.[24] and in this work may be partially explained by the different docking methods used. In the model of Wang et al.,[24] the fold-tree-based Rosetta docking method[49] was used. In this work, MD simulation is used as a docking method, where the flexibility of protein backbone is likely accounted for more realistically. Nevertheless, remarkably similar models are obtained with the two different docking methods.

Computational Mutagenesis. The docking simulation of the AahII–$Na_V1.2$ complex suggests that two charged residues, Glu1551 and Arg1626, are involved in binding. However, mutagenesis experiments have shown that the mutation of Glu1551 to an arginine or Arg1626 to a glutamate has minimal effect on toxin binding affinities.[24] Here with computational mutagenesis, we show that the E1551R and R1626E mutations do not impair toxin–channel interactions because the toxin can form salt bridges with alternative residues from the VS domain.

Starting from the bound complex of AahII–$Na_V1.2$, we perform two separate single mutations, E1551R and R1626E, and equilibrate each system without any restraints for 20 ns. At the end of the 20 ns simulation, the Arg62-Glu1551 salt bridge is observed to be replaced by a Arg62-Asp1554 salt bridge in the AahII–E1551R $Na_V1.2$ complex, whereas His64(COO^-)-Arg1626 is replaced by His64(COO^-)-Arg1629. Thus, each of the single mutations does not affect the toxin binding significantly. The PMF profile for the unbinding of AahII from the E1551R VS domain is constructed with umbrella sampling (Figure 4). The K_d value derived is 18 nM, comparable to the value of 17 nM for the unbinding of AahII from the wild-type VS domain. Thus, the toxin binds to the wild-type and mutant VS domains with similar affinities, in agreement with experiment.

Spontaneous Binding of δ-Conotoxin to $Na_V1.2$. Similar to scorpion α-toxins, δ-conotoxins have also been shown to inhibit the fast activation of Na_V channels.[5,6] The receptor site of δ-conotoxins on Na_V channels may overlap with that of α-toxins.[50] However, δ-conotoxins are frequently much shorter than α-toxins in sequence. For example, the δ-conotoxin EVIA (DDCIK PYGFC SLPIL KNGLC CSGAC VGVCA DL) consists of 32 amino acids[51] compared to the 64 amino acids of AahII. Considering the relatively small size of EVIA, it may be plausible to simulate the binding of EVIA to $Na_V1.2$ without bias.

We place EVIA (PDB ID 1G1P[51]) 20 Å above the extracellular side of the VS domain of $Na_V1.2$ and allow the toxin bind to the VS domain spontaneously. Figure 6 shows that EVIA forms two salt bridges with $Na_V1.2$ after 30 ns of simulation, which remain intact until the simulation was terminated at 50 ns. The salt bridges formed between EVIA–$Na_V1.2$ are similar to that observed in the AahII–$Na_V1.2$ complex, although the latter forms one more salt bridge (R18-E1613). This result is consistent with experiments,[50] which suggest that α-toxins and δ-conotoxins share the same receptor site. The similar salt bridges observed in the EVIA–$Na_V1.2$ and AahII–$Na_V1.2$ complexes indicate that the distance restraints applied in the docking simulation of AahII–$Na_V1.2$ may be appropriate.

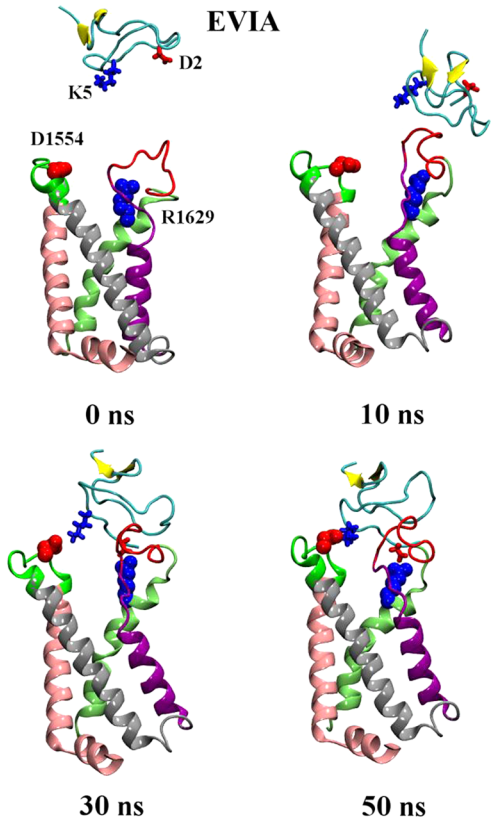

Figure 6. δ-Conotoxin EVIA spontaneously binds to the IVS1-S4 VS-domain of $Na_V1.2$ in a simulation period of 50 ns. Two stable salt bridges, Asp2-Arg1629 and Lys5-Asp1554, are formed.

CONCLUSIONS

Structural models of two α-toxins, AahII and LqhαIT, in complex with the IVS1-S4 VS-domain of $Na_V1.2$ are predicted, with MD simulation as a docking method. The models are built following the hypothesis that anti-mammalian scorpion α- and β-toxins bind to their receptor sites in a similar orientation. The two α-toxins are docked to the receptor site with a functional surface consisting of the NC-, linker- and core-domains. The docked complexes show several electrostatic and hydrophobic interacting residue pairs (Table 2) between each toxin and the VS-domain that are consistent with mutagenesis experiments and can explain why AahII is more effective to $Na_V1.2$ than LqhαIT. Free energy calculations based on the models successfully reproduce the dissociation constants measured experimentally. In addition, δ-conotoxin EVIA binds to $Na_V1.2$ spontaneously over a simulation period of 50 ns, forming two salt bridges similar to that observed in AahII–$Na_V1.2$. The simulations support the hypothesis that scorpion α- and β-toxins share a common binding orientation.

Our model of the AahII–$Na_V1.2$ VS complex can readily predict that several anti-mammalian β-toxins are not suitable to bind the IVS1-S4-domain of $Na_V1.2$. For example, the five-

residue turns (positions 8−12) of the two β-toxins Css4 and Cn2 displayed in Figure 1C do not carry acidic residues and thus are unable to form favorable interactions with the IVS4 helix. In addition, the position 15 in the β-toxins is occupied by a glutamate, similar to that found in anti-insect toxins such as LqhαIT, rendering the insensitivity of the IVS1-S4-domain of $Na_V1.2$ to the β-toxins. Likewise, the models also predict that anti-mammalian α-toxins such as AahII are not suitable to bind the IIS1-S4-domain of $Na_V1.2$, which is the receptor site of β-toxins.

In conclusion, structural models of two scorpion α-toxins in complex with the VS-domain of $Na_V1.2$ are proposed. The models suggest that anti-mammalian α-toxins bind to their receptor sites in an orientation similar to that of β-toxins.

AUTHOR INFORMATION

Corresponding Author

*Tel +61-2-6125-2024; Fax +61-2-6125-0739; e-mail rong.chen@anu.edu.au.

Funding

This work was supported by grants from the National Health and Medical Research Council of Australia. This research was undertaken on the NCI National Facility in Canberra, Australia, which is supported by the Australian Commonwealth Government.

Notes

The authors declare no competing financial interest.

ABBREVIATIONS

COM, center of mass; MD, molecular dynamics; Na_V, voltage-gated sodium; PMF, potential of mean force; VS, voltage sensing.

REFERENCES

(1) Catterall, W. A., Cestele, S., Yarov-Yarovoy, V., Yu, F. H., Konoki, K., and Scheuer, T. (2007) Voltage-gated ion channels and gating modifier toxins. *Toxicon 49*, 124−141.

(2) Stevens, M., Peigneur, S., and Tytgat, J. (2011) Neurotoxins and their binding areas on voltage-gated sodium channels. *Front. Pharmacol. 2*, 71.

(3) Chen, H., Gordon, D., and Heinemann, S. H. (2000) Modulation of cloned skeletal muscle sodium channels by the scorpion toxins Lqh II, Lqh III, and Lqh alphaIT. *Pflügers Arch. 439*, 423−432.

(4) Chen, H., and Heinemann, S. H. (2001) Interaction of scorpion α-toxins with cardiac sodium channels: binding properties and enhancement of slow inactivation. *J. Gen. Physiol. 117*, 505−518.

(5) Barbier, J., Lamthanh, H., Le Gall, F., Favreau, P., Benoit, E., Chen, H., Gilles, N., Ilan, N., Heinemann, S. H., Gordon, D., Ménez, A., and Molgó, J. (2004) A δ-conotoxin from Conus ermineus venom inhibits inactivation in vertebrate neuronal Na^+ channels but not in skeletal and cardiac muscle. *J. Biol. Chem. 279*, 4680−4685.

(6) West, P. J., Bulaj, G., and Yoshikami, D. (2005) Effects of δ-conotoxins PVIA and SVIE on sodium channels in the amphibian sympathetic nervous system. *J. Neurophysiol. 94*, 3916−3924.

(7) Gurevitz, M., Karbat, I., Cohen, L., Ilan, N., Kahn, R., Turkov, M., Stankiewicz, M., Stühmer, W., Dong, K., and Gordon, D. (2007) The insecticidal potential of scorpion β-toxins. *Toxicon 49*, 473−489.

(8) Gordon, D., Karbat, I., Ilan, N., Cohen, L., Kahn, R., Gilles, N., Dong, K., Stuhmer, W., Tytgat, J., and Gurevitz, M. (2007) The differential preference of scorpion α-toxins for insect or mammalian sodium channels: implications for improved insect control. *Toxicon 49*, 452−472.

(9) Bosmans, F., and Tytgat, J. (2007) Voltage-gated sodium channel modulation by scorpion α-toxins. *Toxicon 49*, 142−158.

(10) Housset, D., Habersetzer-Rochat, C., Astier, J. P., and Fontecilla-Camps, J. C. (1994) Crystal structure of toxin II from the scorpion *Androctonus australis* Hector refined at 1.3 Å resolution. *J. Mol. Biol. 238*, 88−103.

(11) Tugarinov, V., Kustanovich, I., Zilberberg, N., Gurevitz, M., and Anglister, J. (1997) Solution structures of a highly insecticidal recombinant scorpion α-toxin and a mutant with increased activity. *Biochemistry 36*, 2414−2424.

(12) Miranda, F., Kupeyan, C., Rochat, H., Rochat, C., and Lissitzky, S. (1970) Purification of animal neurotoxins. Isolation and characterization of eleven neurotoxins from the venoms of the scorpions *Androctonus australis* Hector, *Buthus occitanus tunetanus* and *Leiurus quinquestriatus quinquestriatus*. *Eur. J. Biochem. 16*, 514−523.

(13) Gordon, D., Martin-Eauclaire, M. F., Cestèle, S., Kopeyan, C., Carlier, E., Khalifa, R. B., Pelhate, M., and Rochat, H. (1996) Scorpion toxins affecting sodium current inactivation bind to distinct homologous receptor sites on rat brain and insect sodium channels. *J. Biol. Chem. 271*, 8034−8045.

(14) Benkhadir, K., Kharrat, R., Cestele, S., Mosbah, A., Rochat, H., El Ayeb, M., and Karoui, H. (2004) Molecular cloning and functional expression of the alpha-scorpion toxin BotIII: pivotal role of the C-terminal region for its interaction with voltage-dependent sodium channels. *Peptides 25*, 151−161.

(15) Kahn, R., Karbat, I., Ilan, N., Cohen, L., Sokolov, S., Catterall, W. A., Gordon, D., and Gurevitz, M. (2009) Molecular requirements for recognition of brain voltage-gated sodium channels by scorpion α-toxins. *J. Biol. Chem. 284*, 20684−20691.

(16) Sautière, P., Cestele, S., Kopeyan, C., Martinage, A., Drobecq, H., Doljansky, Y., and Gordon, D. (1998) New toxins acting on sodium channels from the scorpion *Leiurus quinquestriatus hebraeus* suggest a clue to mammalian vs insect selectivity. *Toxicon 36*, 1141−1154.

(17) Eitan, M., Fowler, E., Herrmann, R., Duval, A., Pelhate, M., and Zlotkin, E. (1990) A scorpion-venom neurotoxin paralytic to insects that affects sodium current inactivation: purification, primary structure, and mode of action. *Biochemistry 29*, 5941−5947.

(18) Karbat, I., Kahn, R., Cohen, L., Ilan, N., Gilles, N., Corzo, G., Froy, O., Gur, M., Albrecht, G., Heinemann, S. H., Gordon, D., and Gurevitz, M. (2007) The unique pharmacology of the scorpion α-like toxin Lqh3 is associated with its flexible C-tail. *FEBS J. 274*, 1918−1931.

(19) Tejedor, F. J., and Catterall, W. A. (1988) Site of covalent attachment of α-scorpion toxin derivatives in domain I of the sodium channel α subunit. *Proc. Natl. Acad. Sci. U. S. A. 85*, 8742−8746.

(20) Rogers, J. C., Qu, Y., Tanada, T. N., Scheuer, T., and Catterall, W. A. (1996) Molecular determinants of high affinity binding of α-scorpion toxin and sea anemone toxin in the S3-S4 extracellular loop in domain IV of the Na^+ channel α subunit. *J. Biol. Chem. 271*, 15950−15962.

(21) Benzinger, G. R., Kyle, J. W., Blumenthal, K. M., and Hanck, D. A. (1998) A specific interaction between the cardiac sodium channel and site-3 toxin anthopleurin B. *J. Biol. Chem. 273*, 80−84.

(22) Leipold, E., Lu, S., Gordon, D., Hansel, A., and Heinemann, S. H. (2004) Combinatorial interaction of scorpion toxins Lqh-2, Lqh-3, and LqhαIT with sodium channel receptor sites-3. *Mol. Pharmacol. 65*, 685−691.

(23) Gur, M., Kahn, R., Karbat, I., Regev, N., Wang, J. T., Catterall, W. A., Gordon, D., and Gurevitz, M. (2011) Elucidation of the molecular basis of selective recognition uncovers the interaction site for the core domain of scorpion α-toxins on sodium channels. *J. Biol. Chem. 286*, 35209−35217.

(24) Wang, J. T., Yarov-Yarovoy, V., Kahn, R., Gordon, D., Gurevitz, M., Scheuer, T., and Catterall, W. A. (2011) Mapping the receptor site for α-scorpion toxins on a Na^+ channel voltage sensor. *Proc. Natl. Acad. Sci. U. S. A. 108*, 15426−15431.

(25) Payandeh, J., Scheuer, T., Zheng, N., and Catterall, W. A. (2011) The crystal structure of a voltage-gated sodium channel. *Nature 475*, 353−358.

(26) Zilberberg, N., Froy, O., Loret, E., Cestèle, S., Arad, D., Gordon, D., and Gurevitz, M. (1997) Identification of structural elements of a scorpion α-neurotoxin important for receptor site recognition. *J. Biol. Chem. 272*, 14810−14816.
(27) Karbat, I., Frolow, F., Froy, O., Gilles, N., Cohen, L., Turkov, M., Gordon, D., and Gurevitz, M. (2004) Molecular basis of the high insecticidal potency of scorpion α-toxins. *J. Biol. Chem. 279*, 31679−31686.
(28) Chen, R., and Chung, S. H. (2012) Conserved functional surface of anti-mammalian scorpion β-toxins. *J. Phys. Chem. B 116*, 4796−4800.
(29) Guex, N., and Peitsch, M. C. (1997) SWISS-MODEL and the Swiss-PdbViewer: an environment for comparative protein modeling. *Electrophoresis 18*, 2714−2723.
(30) Schwede, T., Kopp, J., Guex, N., and Peitsch, M. C. (2003) SWISS-MODEL: an automated protein homology-modeling server. *Nucleic Acids Res. 31*, 3381−3385.
(31) Arnold, K., Bordoli, L., Kopp, J., and Schwede, T. (2006) The SWISS-MODEL Workspace: a web-based environment for protein structure homology modeling. *Bioinformatics 22*, 195−201.
(32) Hillisch, A., Pineda, L. F., and Hilgenfeld, R. (2004) Utility of homology models in the drug discovery process. *Drug Discovery Today 9*, 659−669.
(33) Chakrapani, S., Cuello, L. G., Cortes, D. M., and Perozo, E. (2008) Structural dynamics of an isolated voltage-sensor domain in a lipid bilayer. *Structure 16*, 398−409.
(34) Catterall, W. A. (1977) Membrane potential-dependent binding of scorpion toxin to the action potential Na^+ ionophore. Studies with a toxin derivative prepared by lactoperoxidase-catalyzed iodination. *J. Biol. Chem. 252*, 8660−8668.
(35) Mozhayeva, G. N., Naumov, A. P., Nosyreva, E. D., and Grishin, E. V. (1980) Potential-dependent interaction of toxin from venom of the scorpion *Buthus eupeus* with sodium channels in myelinated fibre: voltage clamp experiments. *Biochim. Biophys. Acta 597*, 587−602.
(36) Benoit, E., and Dubois, J. M. (1987) Properties of maintained sodium current induced by a toxin from *Androctonus* scorpion in frog node of Ranvier. *J. Physiol. 383*, 93−114.
(37) Chen, H., Gordon, D., and Heinemann, S. H. (2000) Modulation of cloned skeletal muscle sodium channels by the scorpion toxins Lqh II, Lqh III, and LqhαIT. *Pflügers Arch. 439*, 423−432.
(38) Phillips, J. C., Braun, R., Wang, W., Gumbart, J., Tajkhorshid, E., Villa, E., Chipot, C., Skeel, R. D., Kalé, L., and Schulten, K. (2005) Scalable molecular dynamics with NAMD. *J. Comput. Chem. 26*, 1781−1802.
(39) MacKerell, A. D., Bashford, D., Bellott, M., Dunbrack, R. L., Evanseck, J. D., Field, M. J., Fischer, S., Gao, J., Guo, H., Ha, S., Joseph-McCarthy, D., Kuchnir, L., Kuczera, K., Lau, F. T. K., Mattos, C., Michnick, S., Ngo, T., Nguyen, D. T., Prodhom, B., Reiher, W. E., Roux, B., Schlenkrich, M., Smith, J. C., Stote, R., Straub, J., Watanabe, M., Wiórkiewicz-Kuczera, J., Yin, D., and Karplus, M. (1998) All-atom empirical potential for molecular modeling and dynamics studies of proteins. *J. Phys. Chem. B 102*, 3586−3616.
(40) Klauda, J. B., Venable, R. M., Freites, J. A., O'Connor, J. W., Tobias, D. J., Mondragon-Ramirez, C., Vorobyov, I., MacKerell, A. D., Jr., and Pastor, R. W. (2010) Update of the CHARMM all-atom additive force field for lipids: validation on six lipid types. *J. Phys. Chem. B 114*, 7830−7843.
(41) Jorgensen, W. L., Chandrasekhar, J., Madura, J. D., Impey, R. W., and Klein, M. L. (1982) Comparison of simple potential functions for simulating liquid water. *J. Chem. Phys. 79*, 926−935.
(42) Ryckaert, J. P., Ciccotti, G., and Berendsen, H. J. C. (1977) Numerical integration of the cartesian equations of motion of a system with constraints: molecular dynamics of *n*-alkanes. *J. Comput. Phys. 23*, 327−341.
(43) Miyamoto, S., and Kollman, P. A. (1992) SETTLE: An analytical version of the SHAKE and RATTLE algorithm for rigid water models. *J. Comput. Chem. 13*, 952−962.
(44) Kumar, S., Bouzida, D., Swendsen, R. H., Kollman, P. A., and Rosenberg, J. M. (1992) The weighted histogram analysis method for free-energy calculations on biomolecules. I. The method. *J. Comput. Chem. 13*, 1011−1021.
(45) Allen, T. W., Andersen, O. S., and Roux, B. (2004) Energetics of ion conduction through the gramicidin channel. *Proc. Natl. Acad. Sci. U. S. A. 101*, 117−122.
(46) Chen, R., Robinson, A., Gordon, D., and Chung, S. H. (2011) Modeling the binding of three toxins to the voltage-gated potassium channel (Kv1.3). *Biophys. J. 101*, 2652−2660.
(47) Eriksson, M. A., and Roux, B. (2002) Modeling the structure of agitoxin in complex with the *Shaker* K^+ channel: a computational approach based on experimental distance restraints extracted from thermodynamic mutant cycles. *Biophys. J. 83*, 2595−2609.
(48) Legros, C., Ceard, B., Vacher, H., Marchot, P., Bougis, P. E., and Martin-Eauclaire, M. F. (2005) Expression of the standard scorpion alpha-toxin AaH II and AaH II mutants leading to the identification of some key bioactive elements. *Biochim. Biophys. Acta 1723*, 91−99.
(49) Wang, C., Bradley, P., and Baker, D. (2007) Protein-protein docking with backbone flexibility. *J. Mol. Biol. 373*, 503−519.
(50) Leipold, E., Hansel, A., Olivera, B. M., Terlau, H., and Heinemann, S. H. (2005) Molecular interaction of δ-conotoxins with voltage-gated sodium channels. *FEBS Lett. 579*, 3881−3884.
(51) Volpon, L., Lamthanh, H., Barbier, J., Gilles, N., Molgo, J., Menez, A., and Lancelin, J. M. (2004) NMR solution structures of δ-conotoxin EVIA from *Conus ermineus* that selectively acts on vertebrate neuronal Na^+ channels. *J. Biol. Chem. 279*, 21356−21366.
(52) Pintar, A., Possani, L. D., and Delepierre, M. (1999) Solution structure of toxin 2 from *centruroides noxius* Hoffmann, a β-scorpion neurotoxin acting on sodium channels. *J. Mol. Biol. 287*, 359−367.